Journal of Inorganic Biochemistry 190 (2019) 38–44

Contents lists available at ScienceDirect

Journal of Inorganic Biochemistry

journal homepage: www.elsevier.com/locate/jinorgbio

Anticancer copper complex with nucleus, mitochondrion and cyclooxygenase-2 as multiple targets

Xiangchao Shi[a], Hongbao Fang[a], Yan Guo[a], Hao Yuan[a], Zijian Guo[a,*], Xiaoyong Wang[b,*]

[a] State Key Laboratory of Coordination Chemistry, School of Chemistry and Chemical Engineering, Nanjing University, Nanjing 210023, PR China
[b] State Key Laboratory of Pharmaceutical Biotechnology, School of Life Sciences, Nanjing University, Nanjing 210023, PR China.

ARTICLE INFO

Keywords:
Copper complex
Anticancer drug
Antiinflammation
Mitochondrion
Cyclooxygenase-2

ABSTRACT

Copper complexes are hopeful anticancer drugs due to their multifacet biological properties and high biocompatibility. Inflammatory environment plays an important role in tumor progression and affects the body response to chemotherapeutic agents. A copper(II) complex CuLA with a phenanthroline derivative N-(1,10-phenanthrolin-5-yl)-nonanamide (L) and two aspirin anions (A) as the ligands was synthesized. CuLA effectively induces mitochondrial dysfunction and promotes early-apoptosis in SKOV-3 cells; moreover, it suppresses the expression of cyclooxygenase-2, a key enzyme involved in inflammatory response, in lipopolysaccharide stimulated RAW 264.7 cells. By contrast, the analogue complex CuL without aspirin ligand shows similar influences on cellular redox homeostasis and cell cycle progression but relatively low cytotoxic activity due to its mild effect on mitochondrial function; more importantly, it lacks inhibition to cyclooxygenase-2. The results demonstrate that CuLA inhibits cancer cells through dual pathways involving DNA damage and mitochondrial dysfunction. The introduction of aspirin not only enhances the antitumour efficacy but also reduces the inflammatory threat. Copper complexes with both antitumor and anti-inflammatory activities may represent a new type of multifunctional metal complexes in hope to be developed into novel metallodrugs.

1. Introduction

The discovery of cisplatin declared the commencement of an era for metal-based anticancer drugs [1]. Great attention has been placed on the pharmaceutical properties of metal complexes ever since. A variety of metal complexes, such as those of Pt, Pd, Au and Ru have been designed as anticancer agents and developed for clinical applications [2,3]. As an essential trace element in the human body, copper plays vital functions in various metalloproteins [4]. In 1979, Sigman et al. found that $[Cu(phen)_2]^{2+}$ (phen = 1,10-phenanthroline) is an effective chemical nuclease [5,6], suggesting that copper complexes may have some impact on inhibiting DNA replication in the proliferation of cancer cells. Afterwards, the research of copper complexes made much progress in the anticancer aspect [7]. For example, the success of disulfiram in the clinical trial is mainly attributed to its metabolite, a copper-diethyldithiocarbamate complex, which binds NPL4 and induces its aggregation to kill the cells [8]. We found recently that a series of phenanthroline copper(II) complexes showed potent anti-metastatic and anti-angiogenic activities against cancer cells [9]. These and many other studies show that copper complexes are promising candidates for anticancer drugs.

Chronic inflammation has been recognized as a hallmark of cancers [10], which may be responsible for nearly 15% of all cancers. Inflammatory microenvironment implies poor prognosis and promotion of tumor growth or dissemination; more seriously, it may alter the body response to hormone and chemotherapy [11–13]. Currently, a large proportion of clinical anticancer agents are cytotoxic drugs; however, side effects including necrosis and tissue injury may cause severe inflammatory response and hence induce tumor relapse and drug resistance [14]. These disadvantages stimulate us to develop a combinational drug with both anti-inflammatory and anticancer properties. Actually, the combination of anticancer and anti-inflammatory therapies is becoming a new strategy for cancer treatment. For example, Cu(II)-phenanthroline complexes containing indomethacin can effectively kill the cyclooxygenase-2 (COX-2)-overexpressed breast cancer stem cells [15]; an aspirin-ligated platinum(IV) complex can release cisplatin and aspirin to overcome the side effects and drug resistance of chemotherapy, where the released cisplatin acts on nuclear DNA and aspirin inhibits COX enzyme, controlling the levels of inflammatory responses in tumor-associated macrophages [16,17]. Moreover, Metal complexes could potentiate antitumor activity through interfering with the mitochondrial function of cancer cells [18,19].

* Corresponding authors.
E-mail addresses: zguo@nju.edu.cn (Z. Guo), boxwxy@nju.edu.cn (X. Wang).

https://doi.org/10.1016/j.jinorgbio.2018.10.003
Received 3 August 2018; Received in revised form 9 October 2018; Accepted 12 October 2018
Available online 15 October 2018
0162-0134/

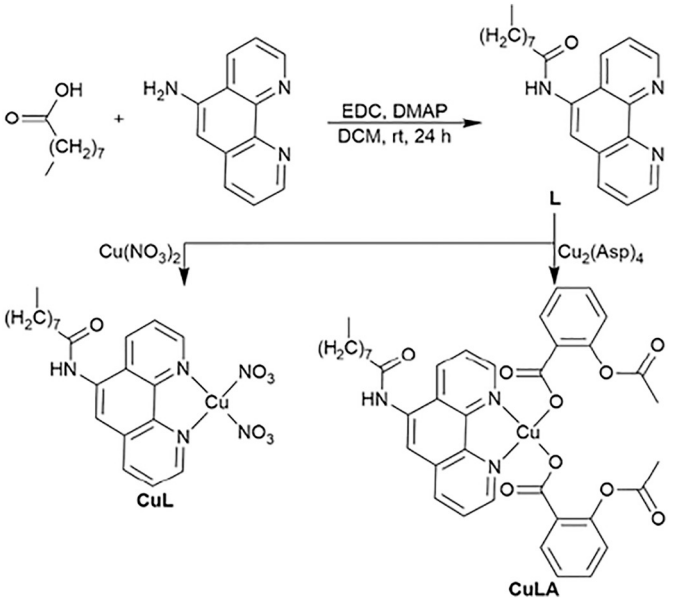

Scheme 1. Synthetic route to ligand L and copper complexes. Asp stands for aspirin.

Aspirin is a globally used non-steroidal anti-inflammatory drug, which can reduce prostaglandin production through COX-2 inhibitory mechanism [20]. Besides, aspirin is reported to play a significant role in the prevention of cardiovascular disease and cancer [21]. Since copper (II) complexes are rich in structural diversity and easy for functional modifications, aspirin may act as an ideal binding partner to form multifunctional combos.

Herein, we report the synthesis and anticancer property of a copper (II) complex CuLA with phen derivative N-(1,10-phenanthrolin-5-yl)-nonanamide (L) and aspirin anions (A) as the ligands, using its analogue CuL without aspirin as a reference (Scheme 1). Both complexes effectively cleave DNA and inhibit the proliferation of cancer cells. The cellular redox homeostasis is greatly disturbed by the complexes. Furthermore, CuLA induces mitochondrial dysfunction and promotes early apoptosis of cancer cells; it also inhibits the expression of COX-2 in lipopolysaccharide (LPS) stimulated macrophages. The remarkable properties of CuLA demonstrate that aspirin-ligated copper complex could play multiple roles in the anticancer action.

2. Results and discussion

2.1. Preparation and characterization

The phen derivative with a long alkyl chain was synthesized to enhance the molecular lipophilicity, which could facilitate the transmembrane ability of the compound. The ligand is characterized by NMR and HRMS spectrometry as shown in Figs. S1–3. CuLA was synthesized by reacting ligand L with $Cu_2(Asp)_4$ in acetonitrile as shown in Scheme 1. CuLA was isolated as a green solid and characterized by HRMS spectrometry (Fig. S4), elemental analysis and ICP-MS (Table S1). CuL was synthesized by reacting cupric salt with ligand L in acetonitrile and characterized by HRMS spectrometry (Fig. S5), elemental analysis and ICP-MS (Table S1). The stability of CuLA and CuL was studied by UV–Vis spectroscopy (Fig. S6). The results show that both complexes are stable in cell culture media over a period of 48 h at 37 °C. The absorption intensity of CuLA was decreased after incubation with cell lysate for 48 h, which suggested that aspirin was released from CuLA under the attack of biomolecules in the cell lysate.

Table 1
IC_{50} values (μM) of compounds against different cell lines at 48 h.

Compounds	SKOV-3	HeLa	HK-2
CuLA	1.1 ± 0.6	1.5 ± 0.5	4.4 ± 0.5
CuL	1.5 ± 0.4	1.8 ± 0.5	4.6 ± 0.8
L	5.4 ± 1.2	6.8 ± 1.2	12.3 ± 1.6

2.2. Cytotoxicity

The cytotoxicity of CuLA, CuL and L was investigated in the human ovarian (SKOV-3) and human cervical (HeLa) cancer cell lines, and the human kidney proximal tubule epithelial (HK-2) cell line. The half maximal inhibitory concentration (IC_{50}) values of the compounds at 48 h are summarized in Table 1. CuLA and CuL displayed strong cytotoxicity to both cancer cell lines. Particularly, CuLA is highly cytotoxic against the SKOV-3 cells, with an IC_{50} value much lower than that of cisplatin (7.08 μM) [18]. Meanwhile, both copper complexes seem to be less detrimental to the HK-2 normal cells. By contrast, the ligand L showed relatively weak cytotoxicity toward all the tested cell lines.

2.3. Cellular uptake and subcellular distribution

The cellular uptake of CuLA and CuL in SKOV-3 cells in terms of Cu was determined by using ICP-MS. As shown in Fig. 1, cellular Cu content was apparently elevated after treatment with both complexes, indicating that the complexes can readily get into the cancer cells due to the alkyl chain. It is consistent with the conclusion that alkyl chain can increase the hydrophobicity of a compound and facilitate its penetration through biological membranes [22]. We further explored the subcellular distribution of the complexes in mitochondria and nuclei. The modification of CuL by aspirin not only increased the cellular Cu content but also increased the mitochondrial Cu content, in that the Cu content ratio of mitochondria to nuclei is 0.86 after the treatment with CuLA, while that is 0.45 after the treatment with CuL at the same condition. The mitochondrial accumulation of CuLA is higher than that of CuL, suggesting that they may cause distinctive disturbances to the mitochondrial function of cancer cells. By contrast, the nuclear accumulation of CuLA is somewhat lower than that of CuL.

2.4. Redox property and DNA cleavage

Redox property is the main character of copper(II) complexes, which may disturb the intracellular homeostasis and kill cancer cells [23,24]. The level of cellular reactive oxygen species (ROS) was thus determined using the 2′,7′-dichloro-dihydrofluorescin diacetate (DCFH-DA) probe. As shown

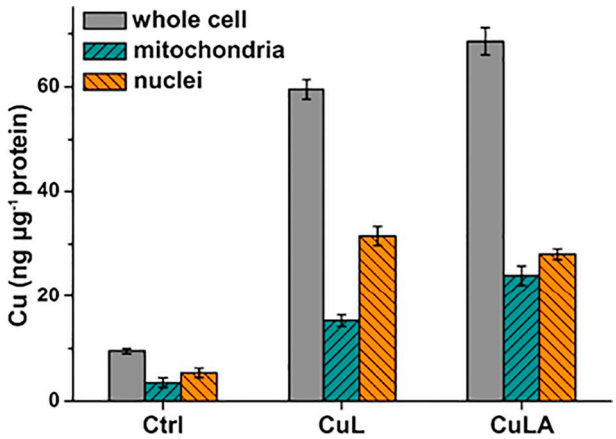

Fig. 1. Cellular and subcellular uptake of CuLA and CuL (2 μM) in SKOV-3 cells after incubation for 24 h.

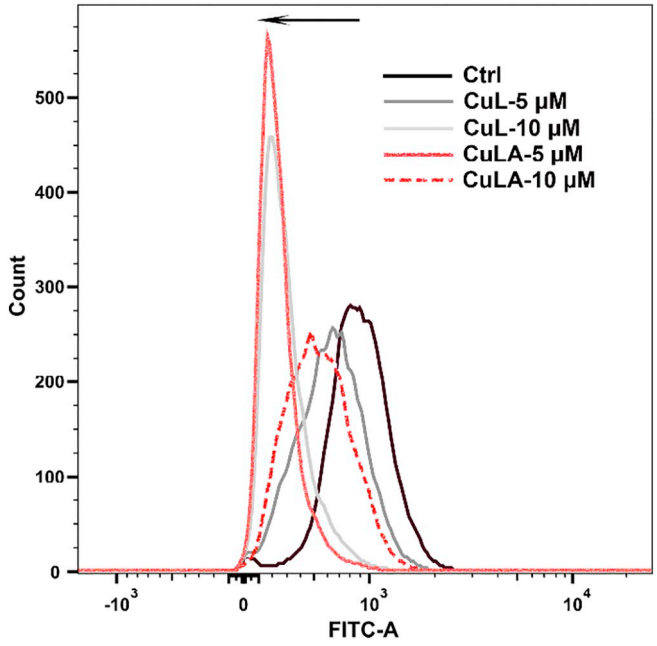

Fig. 2. Cellular ROS level in SKOV-3 cells after incubation with CuLA and CuL (5, 10 μM) for 6 h determined by flow cytometer using the DCFH-DA probe.

in Fig. 2, the mean fluorescence intensities in the cells treated by CuLA (581, 255) and CuL (686, 306) are obviously lower than that in the control cells (966), which suggest that the production of ROS was suppressed by these complexes. CuLA and CuL induced similar dose-dependent decreases in ROS level due to the similar redox copper centre. It is known that in diverse type of cancer cells the level of ROS increases, which play a key role in tumor progression and drug resistance [25]. The alleviation of oxidative stress in cancer cells may slow down the malignant development of tumors [26,27]. Since CuLA and CuL have a great influence on the redox homeostasis of SKOV-3 cells, they may affect the physiological function of cancer cells.

On the other side, ROS is the major destructive factor of DNA; so the DNA cleavage activity of CuLA and CuL was tested by reaction with supercoiled plasmid pUC19 DNA in the presence of reductant ascorbic acid (Vc). As shown in Fig. 3, both complexes show similar cleavage abilities toward supercoiled (Form I) DNA, scissoring it into nicked (Form II) and linear (Form III) DNA. The high cleavage activity may contribute to their strong cytotoxicity.

2.5. Cell cycle

The inhibitory effect of CuLA and CuL on the cell proliferation was reflected on the cell cycle progression. As shown in Fig. 4, incubation of

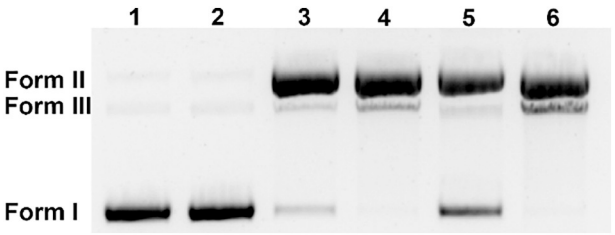

Fig. 3. Cleavage patterns of pUC19 DNA (0.2 μg) by CuL and CuLA in the agarose gel electrophoresis in the presence of ascorbic acid (1 mM) in buffer (50 mM Tris–HCl/50 mM NaCl, pH 7.4) after reaction at 37 °C for 2 h. Lane 1: DNA; Lane 2: DNA + Vc; Lane 3: DNA + Vc + CuL (5 μM); Lane 4: DNA + Vc + CuL (10 μM); Lane 5: DNA + Vc + CuLA (5 μM); Lane 6: DNA + Vc + CuLA (10 μM).

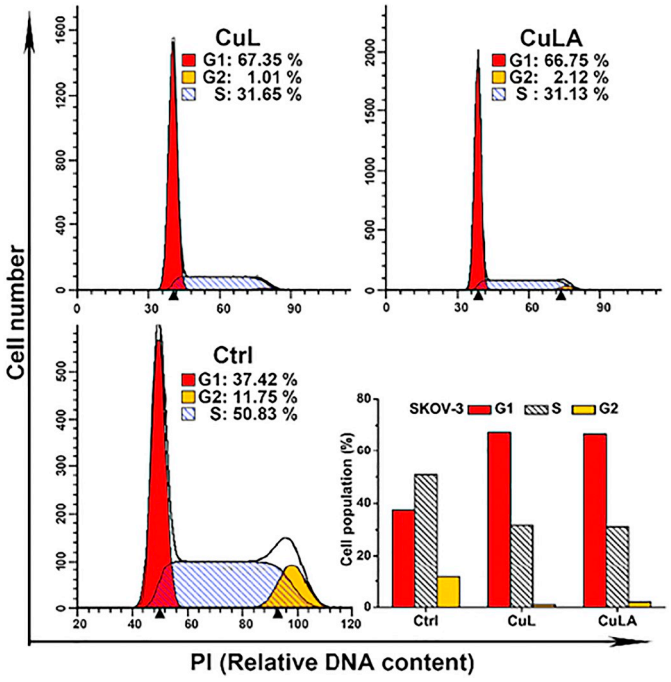

Fig. 4. Cell cycle analysis of SKOV-3 cells after treatment with CuLA and CuL (2 μM) respectively for 24 h.

SKOV-3 cells with CuLA results in a significant cell arrest (ca 67%) at the G1 phase, which suggests that most of the CuLA-treated cells could not enter the S phase. Similar result was observed for the CuL-treated SKOV-3 cells. The results imply that both CuLA and CuL influence the biosynthesis of RNA and protein in the cancer cells, which is an alternative way to suppress the proliferation of cells.

2.6. Apoptosis

Externalization of phosphatidylserine on the outer surface of plasma membrane is the main hallmark in the early-phase of apoptosis [28]. Thus, SKOV-3 cells were stained with Annexin V-FITC (fluorescein isothiocyanate) after treatment with CuLA and CuL, respectively, and phosphatidylserine was detected by flow cytometry. As shown in Fig. 5A, the Annexin V-positive cells treated with CuLA increased by

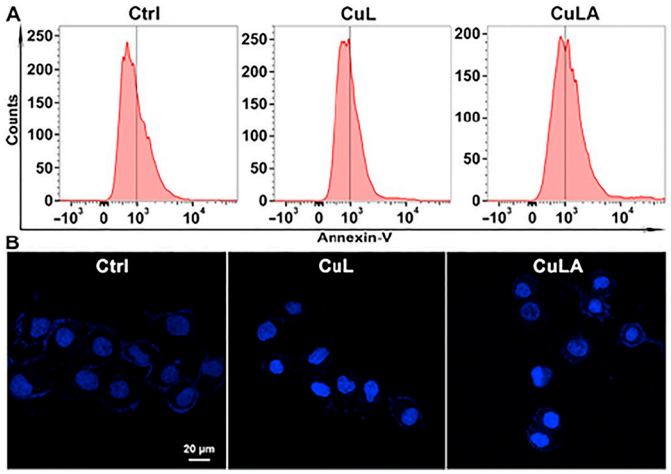

Fig. 5. Early-phase apoptosis of SKOV-3 cells after incubation with CuL or CuLA (5 μM) for 12 h and Annexin V staining (A), and late-phase apoptosis of SKOV-3 cells after incubation with CuL or CuLA (5 μM) for 12 h and Hoechst 33342 staining (B).

70% compared to the control group, while those treated with CuL barely changed. The results indicate that CuLA can effectively promote early-apoptosis of cancer cells due to the presence of aspirin. The pro-apoptotic property of CuLA may result in its higher cytotoxicity to SKOV-3 cells.

Nuclear condensation and fragmentation are considered as indicators of late-phase apoptosis, which can be detected by Hoechst 33342 staining. As shown in Fig. 5B, the nuclear morphology of SKOV-3 cells are greatly changed after incubation with CuLA and CuL respectively, where abnormal shape with condensed chromatin was obviously observed. Since CuLA and CuL displayed similar DNA cleavage activity, their effects on the nuclei are almost identical. The above results revealed that CuLA preserved excellent anticancer property after modification by aspirin.

2.7. Mitochondrial function

Oncogenic stimulation and increased metabolic capability in cancer cells could cause severe intrinsic oxidative stress, directly promoting genetic instability and drug resistance [25]. Oxidative phosphorylation (OXPHOS) is an important process by which respiratory enzymes in mitochondria synthesize ATP from ADP. As the by-product of OXPHOS, mitochondrial ROS (superoxide radical) are viewed as important signalling molecules, and high level of mitochondrial ROS activate apoptosis or autophagy pathway to induce cell death [29]. We hence detected the mitochondrial ROS level in SKOV-3 cells after incubation with CuLA and CuL respectively. As shown in Fig. 6A, the mean fluorescence intensities in the cells treated by CuLA (1709) and CuL (1414) are much larger than that in the control cells (862). Evidently, the level of mitochondrial ROS in SKOV-3 cells was greatly increased after treatment with CuLA, which suggests that the enhanced accumulation of CuLA in mitochondria (see Fig. 1) can effectively promote the production of ROS, thereby making an indispensable contribution to the pro-apoptotic property of CuLA. By contrast, the mitochondrial ROS induced by CuL was less prominent.

The mitochondrial membrane potential ($\Delta\Psi_m$) formed during OXPHOS is the main driving force of ATP production; so $\Delta\Psi_m$ and ATP are important parameters to assess the function of mitochondria. We quantified ATP by measuring the luminescence produced in the reaction of ATP with luciferase. The amount of luminescence is directly proportional to the amount of ATP. As shown in Fig. 6B, CuLA leads to a significant decrease of ATP production in SKOV-3 cells, which suggests that the ATP synthesis ability of mitochondria was greatly reduced. Considering the change of mitochondrial ROS, we may infer that CuLA directly influence the OXPHOS in mitochondria. The effect of CuL on the production of ATP is much less than that of CuLA under the same condition.

Mitochondrial membrane depolarization induced by CuL and CuLA was detected by using JC-1 (5,5′,6,6′-tetrachloro-1,1′,3,3′-tetraethyl-imidacarbocyanine iodide) fluorescent probe. Depending on $\Delta\Psi_m$, JC-1 accumulates as a green monomer in the cytoplasm or as red aggregates in the hyperpolarized mitochondria. The shift in fluorescence emission of JC-1 from red to green could indicate the depolarization of mitochondrial membrane. As shown in Fig. 7, the treatment of SKOV-3 cells with CuLA induced a decrease in red fluorescence and an increase in green fluorescence, suggesting that mitochondrial membrane potential was depolarized. It is well known that the decline of $\Delta\Psi_m$ is the early hallmark of apoptosis. The results demonstrate that CuLA brought about a great disturbance to the mitochondrial function and cell survival. CuL also lead to an increase in green fluorescence, but barely influenced the red fluorescence, implying that its impact on the $\Delta\Psi_m$ is weaker than that of CuLA. The more potent interference of CuLA on the function of mitochondria may be attributed to its higher mitochondrial internalization as compared with CuL (see Fig. 1). Since anticancer agents that disturb mitochondrial function have the potential to bypass the resistance mechanisms evolved toward conventional chemotherapeutics [18,30], CuLA might have an edge in overcoming drug resistance. In addition, reducing oxidative stress can prevent the vicious inflammatory cycle [31]. The influence on mitochondrial function has never been reported in other anti-inflammatory drugs.

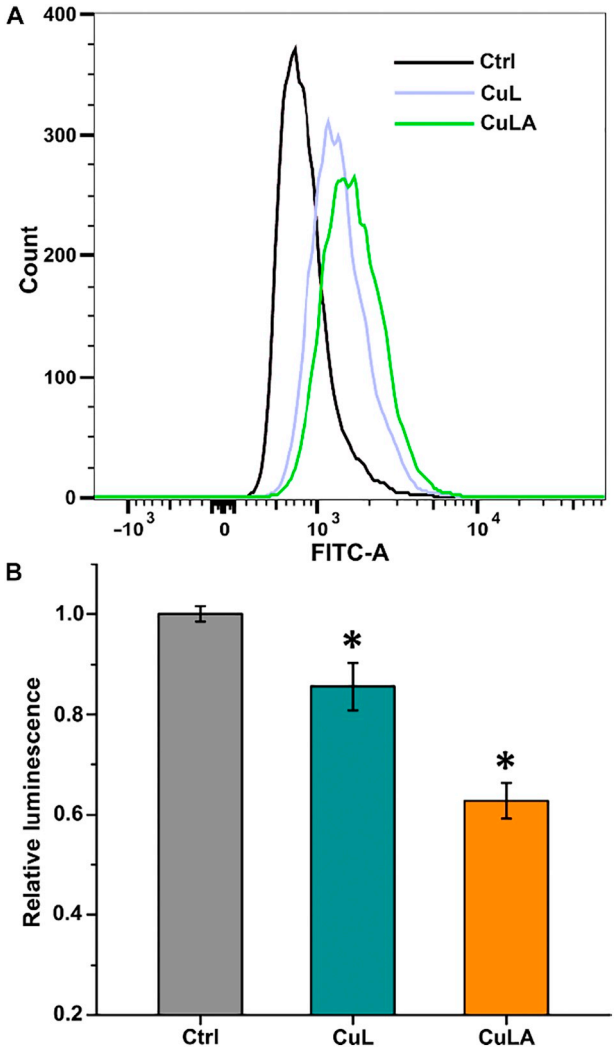

Fig. 6. Mitochondrial ROS (A) and cellular ATP (B) levels in SKOV-3 cells after incubation with CuLA and CuL (5 μM) respectively for 12 h. Data are shown as mean of three independent experiments, * represents $p < 0.05$.

2.8. Inhibition of COX-2 expression

Inflammatory response plays an important part in tumor progression. COX-2 as the key enzyme involved in inflammatory process is considered as the main target of anti-inflammatory drugs. Tumor-associated macrophages are abundantly present in the tumor periphery. The stimulus of exotic pathogen can promote the COX-2 expression in macrophages and trigger chronic inflammation [11–13]. As aspirin is an inhibitor of COX-2, we investigated the COX-2 level in the LPS-stimulated RAW 264.7 macrophages on a flow cytometer after treatment with CuLA and CuL [32,33]. Fig. 8 shows that incubation of LPS-stimulated macrophages with CuL had no influence on the expression of COX-2; however, treatment with CuLA or aspirin suppressed the expression of COX-2. The results reveal that the aspirin-modified CuLA has a potential to prevent inflammation and inhibit tumor proliferation simultaneously.

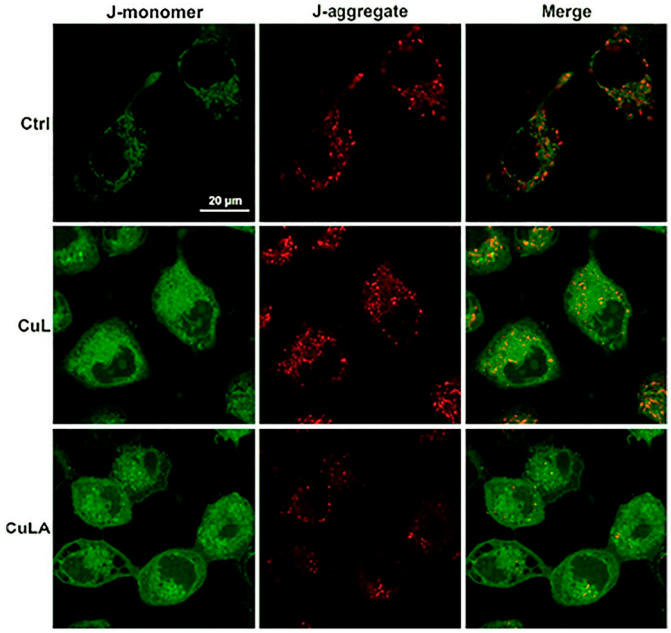

Fig. 7. Mitochondrial membrane potential of SKOV-3 cells indicated by JC-1 staining after incubation with CuL and CuLA (5 μM) respectively for 12 h.

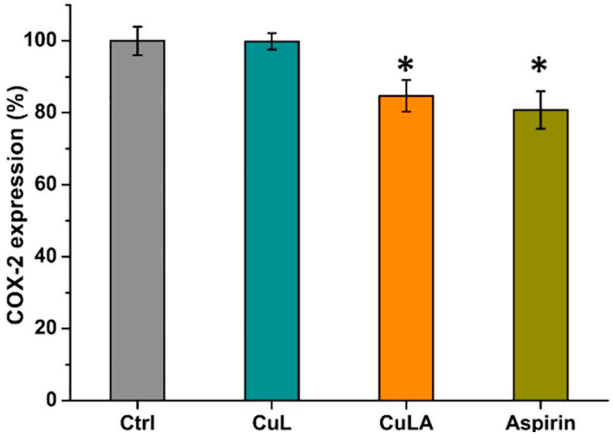

Fig. 8. Histograms of the green fluorescence emitted by RAW 264.7 cells after treating with LPS (1 μg mL^{-1}) for 24 h, incubating with CuL, CuLA (2 μM) and aspirin (4 μM) respectively for 24 h, and staining with anti-COX-2 Alexa Fluor 488 antibody. Data are shown as mean of three independent experiments, * represents $p < 0.05$.

3. Conclusions

We synthesized a copper complex CuLA aiming to inhibit cancer cells in this study. CuLA displayed excellent cytotoxicity and DNA cleavage ability. Relative low level of cellular ROS and conspicuous cell arrest at the G1 phase were observed in the complex-treated SKOV-3 cells. In comparison with the analogue of CuLA, the introduction of aspirin to the copper complex only slightly affected the redox activity of copper(II) centre, but markedly enhanced the mitochondrial accumulation of the complex. As a result, the mitochondrial functions were severely disturbed; and more importantly, aspirin endowed the complex with inhibitory effect on COX-2 in LPS-stimulated macrophages, manifesting its anti-inflammatory potential. Considering the promotive effect of inflammatory cytokines in tumor microenvironment and side effects of traditional platinum-based chemotherapeutics, copper complexes with multiple cellular targets and anti-inflammatory ability may forebode a new trend for the design of anticancer drugs.

4. Experimental section

4.1. Materials

All chemicals were received and used without further purification unless otherwise noted. 1,10-Phenanthrolin-5-amine, nonanoic acid, 1-ethyl-3-(3-dimethylaminopropyl) carbodiimide (EDCI), 4-dimethylaminopyridine (DMAP), and 3-(4,5-dimethylthiazol-2-yl)-2,5-diphenyltetrazolium bromide (MTT) were purchased from Energy Chemical. Copper(II) aspirinate [$Cu_2(Asp)_4$] was prepared according to the literature [34]. COX-2 antibody was purchased from CST (13596). Lipopolysaccharides from Escherichia coli O111:B4 was purchased from Sigma (L2630).

4.2. Measurements

^1H and ^{13}C NMR spectra were recorded on a Bruker Avance DRX-400 with TMS as the internal reference. High resolution mass spectrometric data were determined using an Agilent 6540Q-TOF HPLC-MS spectrometer and the isotopic distribution patterns of the observed species were simulated using Isopro 3.0 program. The inductively coupled plasma mass spectrometry (ICP-MS) data were obtained on ELAN9000 ICP-MS (PerkinElmer). Distilled water was purified by a Millipore water purification system (18.2 MΩ) containing a 0.22 μm filter. The significance of data (p value) was evaluated using GraphPad Prism 6, and the false discovery rate was set to 5%.

4.3. Synthesis of N-(1,10-phenanthrolin-5-yl)nonanamide (L)

1,10-Phenanthrolin-5-amine (0.5 g, 2.56 mmol) was dissolved in distilled dichloromethane (100 mL) before the solution was cooled to 0 °C. Nonanoic acid (0.4 g, 2.56 mmol), EDCI (1.23 g, 6.4 mmol) and DMAP (0.31 g, 2.56 mmol) were added sequentially before the reaction mixture was stirred at 0 °C for another hour. The mixture was allowed to react at room temperature and stirred for 24 h. The solvent was removed under reduced pressure and then purified by silica gel column chromatography using gradient elution of CH_2Cl_2/CH_3OH (0 to 10%). Yield: 0.38 g (47%). ^1H NMR (400 MHz, $CDCl_3$) δ: 9.08 (dd, 2H), 8.29 (s, 1H), 8.11 (dd, 2H), 7.57 (dd, 2H), 2.55 (m, 2H), 1.82 (m, 3H), 1.29 (m, 10H), 0.89 (m, 3H). ^{13}C NMR (100 MHz, $CDCl_3$), 172.59, 150.00, 149.54, 146.08, 143.98, 136.15, 128.36, 124.21, 123.51, 122.79, 119.89, 37.57, 29.37, 29.17, 25.75, 22.65, 14.11. HRMS found (calcd) for $C_{21}H_{24}N_3O$ (m/z): $[M–H]^-$, 334.1903 (334.1919).

4.4. Synthesis of complexes

CuL was prepared by reacting $Cu(NO_3)_2{\cdot}3H_2O$ (20 mg, 0.12 mmol) with ligand L (33 mg, 0.1 mmol) in acetonitrile (10 mL) for 5 h under stirring at room temperature. The blue precipitate was filtered after diethyl ether was added drop wise. The precipitate was recrystallized from acetone and dried in vacuum. HRMS found (calcd) for $C_{21}H_{25}CuN_6O_{10}$ (m/z): $[L + Cu + 3NO_3]^-$, 584.0884 (584.0928). EA found (calcd) for $C_{21}H_{25}CuN_5O_7$: C, 48.03 (48.23); H, 4.77 (4.82); N, 13.23 (13.39); O, 21.20 (21.41).

CuLA was prepared by reacting $Cu_2(Asp)_4$ (80 mg, 0.1 mmol) with ligand L (66 mg, 0.2 mmol) in acetonitrile (20 mL). The reaction mixture was stirred for 12 h at room temperature. The green precipitate was separated by filtration, washed with acetone and dried in vacuum. HRMS found (calcd) for $C_{39}H_{38}CuN_3O_9$ (m/z): $[L–H + Cu + 2(Asp)]^-$, 755.1826 (755.1910). EA found (calcd) for $C_{39}H_{39}CuN_3O_9$: C, 61.58 (61.86); H, 5.08 (5.19); N, 5.23 (5.55); O, 18.89 (19.01).

4.5. Cytotoxicity

HeLa, SKOV-3 and HK-2 cells were cultured in MEM, RPMI 1640 and DMEM/F12 (Gibco) respectively with 10% fetal bovine serum

(Gibco) and 1% penicillin/streptomycin (Gibco) at 37 °C in a humidified incubator with 5% CO_2. The cells (5000–10,000 cells/well) were seeded respectively on a 96-well plate (Corning) in 100 μL medium and incubated at 37 °C in a humidified incubator with 5% CO_2 overnight. The cells were treated with each compound at different concentrations. After incubation for 48 h, the cells were treated with MTT (20 μL, 5 mg mL^{-1} in PBS) for 4 h at 37 °C. The media in each well was replaced by DMSO (200 μL) for solubilization of formazan. The plate was incubated under gentle agitation for 10 min. The optical density (OD) value at 570 nm of each well was measured by microplate reader (Thermo Scientific Varioskan Flash). Each well was performed in triplicate. The mean of three independent results was taken as the inhibition rate (%) or IC_{50} (μM).

4.6. Cellular and mitochondrial uptake

SKOV-3 cells were seeded in a 6-well plate (Corning) at a density of 10^5 cells mL^{-1} and incubated overnight to 60–70% confluence. The cell culture medium was replaced with fresh growth medium and the cells were treated with CuL and CuLA (2 μM) respectively for 24 h. The cells were harvested, trypsinized and washed with PBS. The concentration of protein was determined after lysis buffer (KeyGEN BioTECH) was added to the cell precipitate. The cell lysis solution was digested by concentrated nitric acid (100 μL) at 95 °C for 2 h, hydrogen peroxide (30%, 50 μL) at 95 °C for 1.5 h and concentrated hydrochloric acid (50 μL) at 37 °C until the total volume is < 50 μL. Distilled water was added to each sample to adjust the solution volume to 1 mL. The Cu content in each sample was tested by ICP-MS.

SKOV-3 cells were seeded into 10 cm petri dish. Mitochondria were isolated by a mitochondrial isolation kit (Beyotime Biotechnology). After the same treatment as described above, the cell precipitate was suspended in the mitochondrial isolation solution (0.6 mL) and cooled in ice for 10 min. The cell suspension was homogenized and centrifuged at 600*g* for 10 min to obtain nucleus precipitate. The supernatant was transferred to another tube and centrifuged at 11000*g* for 10 min. The mitochondrial precipitate was collected. The processes of digestion and Cu detection were the same as described above.

4.7. Determination of cellular and mitochondrial ROS

The production of cellular and mitochondrial ROS was measured using the fluorescent probe DCFH-DA (KeyGEN BioTECH) and MitoSOX (Invitrogen) respectively. SKOV-3 cells were seeded in a 6-well plate (Corning) at a density of 10^5 cells mL^{-1} and incubated overnight to 60–70% confluence. After incubation with CuL and CuLA (5, 10 μM) respectively for different hours, the cells were washed and incubated with incomplete growth medium under 1 μM of probe at 37 °C for 30 min in situ. The cells were trypsinized, washed with PBS and resuspended in 500 μL PBS. Analysis was performed on the BD FACSCalibur flow cytometer within 1 h.

4.8. DNA cleavage

Plasmid DNA (pUC19) was purchased from Invitrogen. The solution of plasmid pUC19 DNA (0.2 μg) were incubated with the solution of ascorbic acid (1 mM), complex CuL or CuLA (5, 10 μM) at 37 °C for 2 h in buffer (50 mM Tris-HCl/50 mM NaCl buffer, pH 7.4, total 10 μL). Electrophoresis was performed as described earlier [9].

4.9. Cell cycle analysis

SKOV-3 cells were seeded in a 6-well plate (Corning) at a density of 10^5 cells mL^{-1} and incubated overnight to 40–50% confluence. After incubation with CuL and CuLA (2 μM) respectively for 24 h, the cells were harvested by trypsinization and washed with PBS. The cell precipitation was fixed in 70% ethanol and kept at 4 °C for at least 12 h. The cells were then washed with PBS and incubated with RNAnase (100 μL, KeyGEN BioTECH) in water bath at 37 °C for 1 h. The cells were washed with PBS and stained with PI (400 μL, KeyGEN BioTECH) solution and incubated at room temperature in the dark for 0.5 h. Each sample was washed by PBS and resuspended in PBS (500 μL). Analysis was performed on the BD FACSCalibur flow cytometer within 1 h.

4.10. Apoptotic assay

SKOV-3 cells were seeded in a 6-well plate (Corning) at a density of 10^5 cells mL^{-1} and incubated overnight to 60–70% confluence. The cells were treated with CuL and CuLA (10 μM) respectively for 12 h, trypsinized and washed with PBS. Apoptosis detection kit (BD Biosciences) was used to stain the cells. The cell precipitation was suspended into 1 × binding buffer (100 μL) and Annexin V-FITC (5 μL) was added into the solution and incubated at room temperature for 1 h. Analysis was performed on the BD FACSCalibur flow cytometer within 1 h after 1 × binding buffer (400 μL) was added.

SKOV-3 cells were seeded in a glass bottom cell culture dish (φ 2 mm, NEST) containing 1 mL of growth medium at 40% confluence. The cell culture medium was replaced with fresh growth medium before incubation with CuL and CuLA (10 μM) respectively. The cells were labelled with Hoechst 33342 (2 μg mL^{-1}, KeyGEN BioTECH) for 30 min and then washed thrice with HBSS solution before imaging. The imaging was carried out by confocal laser scanning fluorescence microscopy (Zeiss LSM710) with a 20× objective lens.

4.11. Evaluation of ATP and mitochondrial membrane potential

SKOV-3 cells were seeded in a 6-well plate (Corning) at a density of 10^5 cells mL^{-1} and incubated overnight to 60–70% confluence. Cell culture medium was replaced with fresh growth medium. The cells were treated with CuL and CuLA (5, 10 μM) respectively for 12 h. The cell lysis was centrifuged at 12000 *g* and 4 °C for 5 min. In a 96-well black plate (Corning), the supernatant (20 μL) was added into ATP working solution (100 μL, Beyotime Biotechnology) in triplicate. The luminescence of each well was detected by a microplate reader (Thermo Scientific Varioskan Flash) as soon as possible.

SKOV-3 cells were seeded in a glass bottom cell culture dish (φ 2 mm, NEST) containing 1 mL of growth medium at 40% confluence. The cell culture medium was replaced with fresh growth medium before incubation with CuL and CuLA (5, 10 μM) respectively. A solution of JC-1 reagent (Beyotime Biotechnology) was added and incubated at 37 °C for 20 min. The cells were washed thrice with incomplete culture medium before imaging. The imaging was carried out with a confocal laser scanning fluorescence microscopy (Zeiss LSM710) with a 63× objective lens.

4.12. Detection of cellular COX-2

RAW 264.7 macrophages were cultured in DMEM (Gibco) supplemented with 1% penicillin/streptomycin (Gibco) and 10% heat-inactivated fetal bovine serum (Gibco) at 37 °C in a humidified incubator with 5% CO_2. The cells were seeded in 6-well plates at a density of 5×10^5 cells mL^{-1} and allowed to attach overnight. The cells were pretreated with LPS (1 μg mL^{-1}) for 24 h, and then incubated with each compound for 24 h. The cells were harvested by trypsinization, fixed with 4% paraformaldehyde at 37 °C for 10 min, permeabilized with ice cold methanol for 30 min, and suspended in PBS (200 μL). The Alexa Fluor® 488 labelled anti-COX-2 antibody (5 μL) was added to the cell suspension and incubated in the dark for 1 h. Each sample was washed by PBS and resuspended in PBS (500 μL). Analysis was performed on the BD FACSCalibur flow cytometer within 1 h.

Acknowledgements

This work is supported by the National Natural Science Foundation of China (Grants 31570809, 21877059, and 21731004), the National Basic Research Program of China (Grant 2015CB856300), and the Natural Science Foundation of Jiangsu Province (Grant BK20150054).

Appendix A. Supplementary data

Supplementary data to this article can be found online at https://doi.org/10.1016/j.jinorgbio.2018.10.003.

References

[1] S. Dasari, P.B. Tchounwou, Eur. J. Pharmacol. 740 (2014) 364–378.
[2] X.Y. Wang, Z.J. Guo, Dalton Trans. (2008) 1521–1532.
[3] F. Trudu, F. Amato, P. Vaňhara, T. Pivetta, E.M. Peña-Méndez, J. Havel, J. Appl. Biomed. 13 (2015) 79–103.
[4] R.A. Festa, D.J. Thiele, Curr. Biol. 21 (2011) R877–R883.
[5] D.S. Sigman, D.R. Graham, V. D'Aurora, A.M. Stern, J. Biol. Chem. 254 (1979) 12269–12272.
[6] D.R. Graham, L.E. Marshall, K.A. Reich, D.S. Sigman, J. Am. Chem. Soc. 102 (1980) 5419–5421.
[7] C. Santini, M. Pellei, V. Gandin, M. Porchia, F. Tisato, C. Marzano, Chem. Rev. 114 (2014) 815–862.
[8] Z. Skrott, M. Mistrik, K.K. Andersen, S. Friis, D. Majera, J. Gursky, T. Ozdian, J. Bartkova, Z. Turi, P. Moudry, M. Kraus, M. Michalova, J. Vaclavkova, P. Dzubak, I. Vrobel, P. Pouckova, J. Sedlacek, A. Miklovicova, A. Kutt, J. Li, J. Mattova, C. Driessen, Q.P. Dou, J. Olsen, M. Hajduch, B. Cvek, R.J. Deshaies, J. Bartek, Nature 552 (2017) 194–199.
[9] X.C. Shi, Z.Y. Chen, Y.J. Wang, Z.J. Guo, X.Y. Wang, Dalton Trans. 47 (2018) 5049–5054.
[10] D. Hanahan, R.A. Weinberg, Cell 144 (2011) 646–674.
[11] G. Marelli, A. Sica, L. Vannucci, P. Allavena, Curr. Opin. Pharmacol. 35 (2017) 57–65.
[12] C.I. Diakos, K.A. Charles, D.C. McMillan, S.J. Clarke, Lancet Oncol. 15 (2014) 493–503.
[13] J. Candido, T. Hagemann, J. Clin. Immunol. 33 (2013) 79–84.
[14] S.I. Grivennikov, F.R. Greten, M. Karin, Cell 140 (2010) 883–899.
[15] J.N. Boodram, I.J. Mcgregor, P.M. Bruno, P.B. Cressey, M.T. Hemann, K. Suntharalingam, Angew. Chem. Int. Ed. 55 (2016) 2845–2850.
[16] R.K. Pathak, S. Marrache, J.H. Choi, T.B. Berding, S. Dhar, Angew. Chem. Int. Ed. 53 (2014) 1963–1967.
[17] Q.Q. Cheng, H.D. Shi, H.X. Wang, Y.Z. Min, J. Wang, Y.Z. Liu, Chem. Commun. 50 (2014) 7427–7430.
[18] W. Zhou, X.Y. Wang, M. Hu, C.C. Zhu, Z.J. Guo, Chem. Sci. 5 (2014) 2761–2770.
[19] S.X. Jin, Y.G. Hao, Z.Z. Zhu, N. Muhammad, Z.Q. Zhang, K. Wang, Y. Guo, Z.J. Guo, X.Y. Wang, Inorg. Chem. 57 (2018) 11135–11145.
[20] P. Tosco, L. Lazzarato, Chem. Med. Chem. 4 (2009) 939–945.
[21] M.J. Thun, E.J. Jacobs, C. Patrono, Nat. Rev. Clin. Oncol. 9 (2012) 259–267.
[22] M.P. Murphy, R.A.J. Smith, Annu. Rev. Pharmacol. Toxicol. 47 (2007) 629–656.
[23] G. Filomeni, G. Cerchiaro, A.M. Da Costa Ferreira, A. De Martino, J.Z. Pedersen, G. Rotilio, M.R. Ciriolo, J. Biol. Chem. 282 (2007) 12010–12021.
[24] W.J. Guo, S.S. Ye, N. Cao, J. Huang, J. Gao, Q.Y. Chen, Exp. Toxicol. Pathol. 62 (2010) 577–582.
[25] H. Pelicano, D. Carney, P. Huang, Drug Resist. Updat. 7 (2004) 97–110.
[26] U.K. Udensi, P.B. Tchounwou, J. Exp. Clin. Cancer Res. 35 (2016) 139–157.
[27] G.R. Devi, J.L. Allensworth, M.K. Evans, S.J. Sauer, Cancer (2014) 3–14.
[28] J. Wang, P. Zhang, C. Qian, X. Hou, L. Ji, H. Chao, J. Biol. Inorg. Chem. 19 (2014) 335–348.
[29] S. Vyas, E. Zaganjor, M.C. Haigis, Cell 166 (2016) 555–566.
[30] I.R. Indran, G. Tufo, S. Pervaiz, C. Brenner, Biochim. Biophys. Acta 1807 (2011) 735–745.
[31] M.J. López-Armada, R.R. Riveiro-Naveira, C. Vaamonde-García, M.N. Valcárcel-Ares, Mitochondrion 13 (2013) 106–118.
[32] Y. Sato, Y. Goto, N. Narita, D.S.B. Hoon, Cancer Microenviron. 2 (2009) 205–214.
[33] D.H. Kim, J.H. Chung, J.S. Yoon, Y.M. Ha, S. Bae, E.K. Lee, K.J. Jung, M.S. Kim, Y.J. Kim, M.K. Kim, H.Y. Chung, J. Ginseng Res. 37 (2013) 54–63.
[34] T. Fujimori, S. Yamada, H. Yasui, H. Sakurai, Y. In, T. Ishida, J. Biol. Inorg. Chem. 10 (2005) 831–841.